Int. J. Electrochem. Sci., 16 **(2021)** Article Number: 211027, doi: 10.20964/2021.10.34

International Journal of
ELECTROCHEMICAL
SCIENCE
www.electrochemsci.org

Effect of oleic acid on the corrosion resistance of carbon steel in concrete exposed in NaCl solution

Tao Ji[1,], Shiping Zhang[1], Yan He[2], Weihua Li[3], Fubin Ma[3,*]*

[1] School of Architecture and Civil Engineering, Nanjing Institute of Technology, Nanjing, 211167, China
[2] School of civil engineering, Suzhou University of Science and Technology, Suzhou, 215009, China
[3] Institute of Oceanology, Chinese Academy of Sciences, Qingdao, 266071, China
[*]E-mail: njitjitao@sina.com ; mfb281@163.com

Received: 28 June 2021 / *Accepted:* 4 August 2021 / *Published:* 10 September 2021

Oleic acid was incorporated into concrete to observe its influence on the corrosion resistance of carbon steel in the presence of chloride ions. Penetration tests, concrete pore structure tests, electrochemical experiments and XRD tests were performed to study the inhibition and mechanism of oleic acid on reinforced concrete structures. The obtained results showed that oleic acid performed well in inhibiting the corrosion of carbon steel. The chloride penetrability test resulted in a decreased chloride migration coefficient value when oleic acid was added to the concrete. The increased potential from the open circuit potential test, the increased resistance of the concrete, the increased resistance of the charge transfer process from the electrochemical impedance spectroscopy measurement and the decreased corrosion current density from the polarization curve test revealed that the corrosion of the carbon steel in the concrete was slowed. XRD, the concrete pore structure and the contact angle analysis revealed that the inhibition was mainly due to the reaction of oleic acid and the hydration products of cement.

Keywords: oleic acid; carbon steel; electrochemical techniques; chloride penetration; concrete

1. INTRODUCTION

Reinforced concrete is one of the most commonly used materials in civil engineering construction; due to its excellent mechanical properties, easy availability and low cost [1-3]. The carbon steel inside is usually well-protected by the alkaline environment of the concrete [4, 5]. However, once aggressive media permeate through the concrete and arrive at the carbon steel surface, they accumulate to a certain concentration, and the passive film of carbon steel becomes unstable and begins to corrode [6-10]. Among all aggressive media, chloride ions are the most harmful due to their catalytic effect on the

electrochemical reaction of carbon steel [11, 12].

Damage caused by carbon steel corrosion, such as cracking of the concrete, reduction of the bearing capacity and the crashing of the reinforced structure, has been widely reported previously [13-19]. To reduce the damage caused by carbon steel corrosion, researchers have put much effort into reducing the penetration rate of chloride ions through the concrete, which has been proven to be effective, especially when the concrete structure is in saline-alkali land or used in de-icing and marine environments [20-25]. Various methods have been taken to reduce the penetration rate of chloride ions. For example, Takewaka and Mastumoto adopted a dualistic diffusion equation to explain the relationship between chloride penetration and thickness of concrete and pointed out a thick concrete cover is required to prevent chlorides from reaching the carbon steel [26]. Poon et al. studied the effect of the porosity and pore structure of concrete on chloride diffusivity and found that a lower porosity enhanced the resistance to chloride penetration of concrete [27]. In addition, different methods, such as adding finer powders, more superplasticizer and supplementary cementitious materials, have been used to decrease the porosity and optimize the pore structure of concrete, which could slow the penetration of the chlorides [28-31]. Concrete coatings, including organic and inorganic coatings, can block the capillary pores in the concrete surface and delay the initiation of chloride penetration [32-36]. Although these measures to reduce the penetration rate of chloride ions through concrete have proven effective, some new methods and materials are still needed.

Oleic acid, which is usually used as a waterproofing agent when concrete suffers water attack, performs well in decreasing the permeability of concrete [37-40]. Oleic acid can react with calcium hydroxide, one of the products of cement hydration, and generate oleic acid calcium. Oleic acid calcium is hydrophobic and cannot be wetted easily. Studies on this waterproofing agent that is used to inhibit the penetration of water into concrete structures are extensive. However, its effect on carbon steel corrosion in concrete structures is not clear to our knowledge. The objective of this work is to investigate the effect of oleic acid on the corrosion resistance of carbon steel in concrete structures. For this purpose, oleic acid was incorporated into the concrete to inhibit the corrosion of carbon steel. The corrosion inhibition and mechanism were studied by electrochemical testing, penetration testing and X-ray diffraction (XRD).

2. EXPERIMENTAL

2.1. Materials and sample preparation

The oleic acid used in this work was purchased from Macklin Biochemical Co., Ltd, Shanghai. The oleic acid sample was characterized by FT-IR spectroscopy using KBr pellets (Nicolet IS10 infrared spectrophotometer, USA). The FT-IR transmission spectra is shown in **Fig. 1**. The sharp peaks near 2910 and 1450 cm^{-1} correspond to the stretching and bending vibrations of C–H. The wide absorption peaks near 1300 and 1500 cm^{-1} correspond to the stretching vibrations of $–CH_2$ and $–CH_3$, respectively. The two obtained absorption peaks near 2840 and 930 cm^{-1} correspond to the stretching and bending vibrations of O–H. The sharp peaks near 1700 cm^{-1}, 1570 cm^{-1} and 1180 cm^{-1} correspond to C=O

stretching vibrations, C=C stretching vibrations and C–C stretching vibrations, respectively. Because there were no other absorption peaks, the sample was confirmed to oleic acid from the FT-IR spectroscopy results.

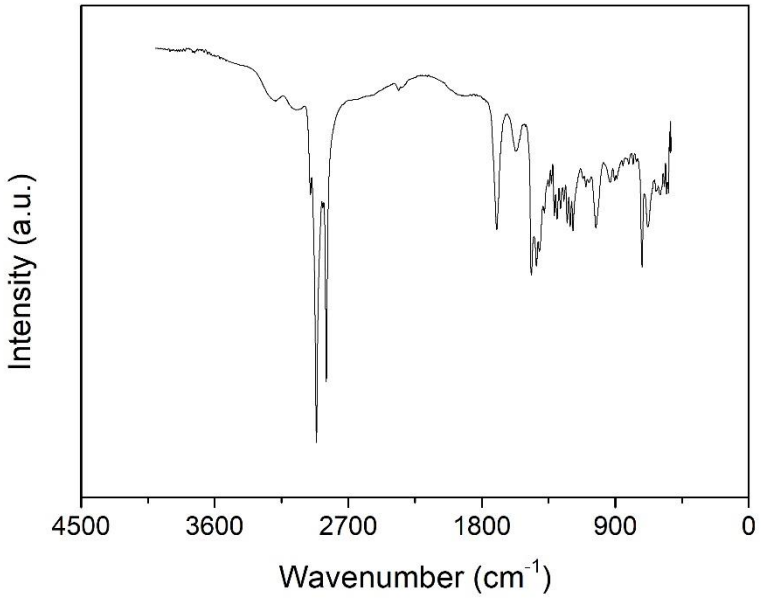

Figure 1. Fourier transform infrared transmission spectra of the oleic acid sample

The carbon steel used for the research in this work was ordinary Q235 carbon steel without ribs. The weight fractions (wt.%) of Mn, Si, C, S, P and Fe were 0.45, 0.23, 0.19, 0.018, 0.0058 and 99.11, respectively. The cylindrical carbon steel specimen had a diameter of 12 mm and a length of 130 mm. Before concrete casting, the carbon steel was pretreated, and the pretreatment included derusting with pickling solution and removal of impurities from the surface by washing with ethanol and drying in an air-circulating oven. Portland cement, water, plasticizer, oleic acid (OA), and fine and coarse aggregates (FA/CA) were used to design the concrete mixtures. The density and specific surface area of the cement used were 3120 $kg \cdot m^{-3}$ and 364 $m^2 \cdot kg^{-1}$, respectively. The chemical compositions of the cement used are listed in Table 1. The polycarboxylate superplasticizer with 22% solid content exhibited a water reducing rate of 25%.

Table 1. Compositions of the used portland cement

Composition	SiO_2	Fe_2O_3	Al_2O_3	CaO	MgO	SO_3	K_2O	Na_2O	TiO_2	P_2O_5
Content （wt. %）	22.91	3.10	7.35	57.46	4.07	1.52	0.47	0.99	0.35	0.05

Different samples were prepared for the following test and analysis. Plain concrete samples with a diameter of 100 mm and a height of 50 mm were prepared for the rapid chloride penetration test.

Cement paste samples with a size of 40 × 40 × 160 mm were prepared for analysis of cement hydration. Carbon steel electrode in concrete protected by an epoxy resin was prepared for the electrochemical test, as shown in **Fig. 2**. The compositions of the concrete (C0, C1 and C2) and cement paste mixtures (P0 and P1) used are listed in Table 2. All the samples were cured for 28 days with a temperature of 20± 1 °C and a humidity of 90±5% before any test was performed. The carbon steel electrode in concrete was immersed in 10 wt.% NaCl solution to accelerate the corrosion of the embedded carbon steel.

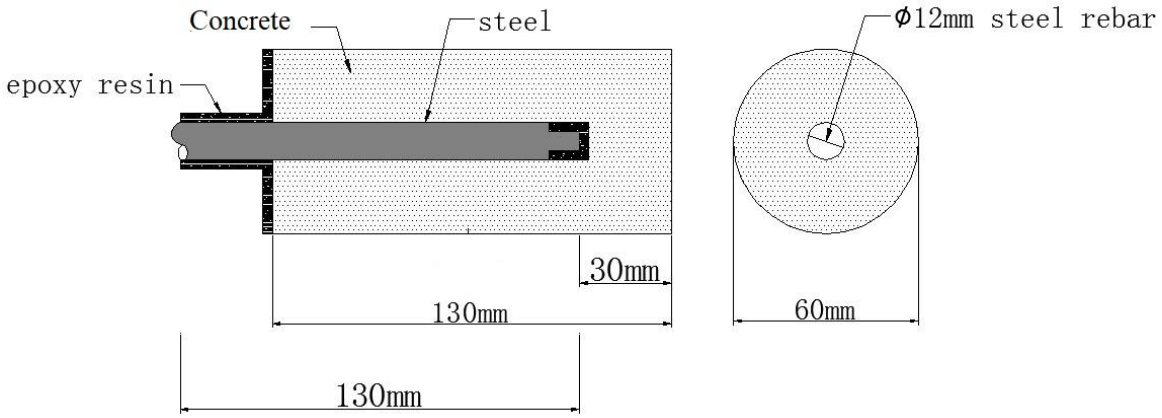

Figure 2. Schematic diagram of the carbon steel electrode in concrete

Table 2. Compositions of the prepared concrete and cement paste mixtures

Series	Cement/kg	Water/kg	Plasticizer/g	OA/g	FA/kg	CA/kg
P0	1.00	0.40	8.0	-	-	-
P1	1.00	0.40	8.0	2.8	-	-
C0	1.00	0.40	8.0	-	1.70	2.10
C1	1.00	0.40	8.0	1.4	1.70	2.10
C2	1.00	0.40	8.0	2.8	1.70	2.10

2.2. Penetration test of concrete samples

Plain, cylindrical concrete samples cured for 28 days with and without the oleic acid were used to test the chloride penetrability of concrete according to NT Build 492–1999. The chloride migration coefficient can be calculated with the following equation:

$$D_{RCM} = \frac{0.0239\times(273+T)L}{(U-2)t}\left(X_d - 0.0238\sqrt{\frac{(273+T)LX_d}{U-2}}\right) \quad (1)$$

where D_{RCM} represents the migration coefficient under non-steady-state conditions ($10^{-12}m^2/s$), U represents the applied voltage (V), t represents the test duration (h), T represents the average temperature of the anolyte solution before and after the test (°C), L represents the thickness of the tested concrete specimen (mm) and X_d represents the average penetration depth (mm).

2.3. Electrochemical experiments

The potential, impedance spectra and polarization curve of the carbon steel electrode in concrete were tested with a PARSTAT 2273 potentiostat/galvanostat. The test system was a three-electrode cell system with the carbon steel electrode in concrete as the working electrode, the saturated calomel electrode (SCE) as the reference electrode and a coiled platinum wire with 10 rings as the counter electrode. All the electrodes were immersed in 10 wt.% NaCl solution when the electrochemical tests were carried out.

The open circuit potential of the specimen was determined first, and the potential value was taken as the corrosion potential when it did not change by more than 2 mV in 300 s. Then electrochemical impedance spectroscopy test carried out with sine wave circuit excitation. Its amplitude was 10 mV peak-to-peak, and its frequency was from 100 kHz to 10 MHz. After that, the polarization curve measurement was carried out with a scan rate of 1 $mV \cdot s^{-1}$ from -250 mV to +250 mV versus the obtained open circuit potential.

2.4. Cement hydration analysis

The effect of oleic acid on the hydration of cement was analysed by X-ray diffraction (XRD) with an Ultima IV diffractometer. The wavelength, tube voltage and tube current of the radiation source from Cu Kα were 1.5418 Å, 40 kV and 40 mA, respectively. The cement hydration sample was prepared as follows: the cement paste sample was crushed and cured for 28 days, and then the hydration process was quenched with absolute ethanol. The sample was ground into a powder and dried at 40 °C until its mass was constant. Scanning of the XRD pattern with angles ranging from 10° to 80° and steps of 0.02° occured after the sample was fully prepared.

2.5. Concrete pore structure test

The concrete samples cured after 28 days were immersed in ethanol for 24 h and then dried for 72 h at 60 °C. Then, they were cut and polished to obtain 100 × 100 × 10 mm concrete slices for the pore structure test. The concrete pore structure was tested by the linear-traverse method according to ASTM C457–2006.

2.6. Contact angle test

To estimate the hydrophobic properties of the oleic acid-modified concrete, 10 μl distilled water was dropped on the surface of the hardened cement paste. Then, the Laplace-Young fitting algorithm was applied to the water-cement paste contact images to calculate the contact angles.

3. RESULTS AND DISCUSSION

3.1. Penetration of concrete samples

The chloride migration coefficients of the concrete samples with different oleic acid contents are listed in Table 3. The chloride migration coefficient of the concrete decreased with increasing oleic acid content inside the sample. The decreased chloride migration coefficient may be partly due to the lower surface tension of the hydration products of cement according to the study of hydrophobic concrete from Al-Kheetan et al [41]. The decreased penetration rate of water decreased the penetration of chloride ions to some extent. It can be concluded that oleic acid can inhibit the migration of chloride ions from the outside environment into concrete.

Table 3. The chloride migration coefficient value of the concrete samples with different oleic acid contents

Series	Cement/kg	Water/kg	Plasticizer/g	FA/kg	CA/kg	WP/g	$D_{RCM}/10^{-12}m^2/s$
C0	1.00	0.40	8.0	1.70	2.10	-	4.50
C1	1.00	0.40	8.0	1.70	2.10	7.0	3.18
C2	1.00	0.40	8.0	1.70	2.10	14.0	1.42

3.2. Open circuit potential (OCP)

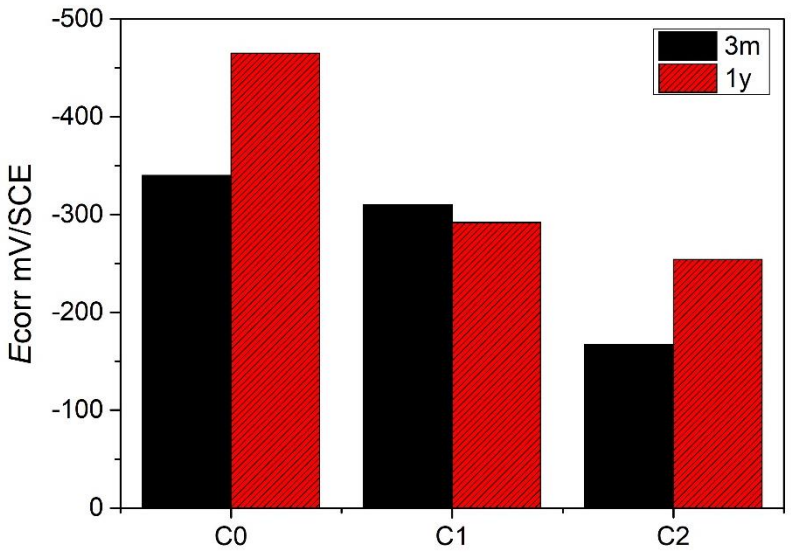

Figure 3. Open circuit potential of the carbon steel electrode in concrete immersed in 10 wt.% NaCl solution for 3 months and 1 year

The open circuit potentials of the reinforced concrete samples with and without oleic acid immersed in 10 wt.% NaCl solution for 3 months and 1 year are shown in **Fig. 3**. It can be seen from the figure that the potential of the carbon steel electrode in concrete increased with increasing content of oleic acid in the concrete. This result reveals that the penetration of Na^+ and Cl^- from the immersion

solution into the concrete decreased with increasing oleic acid content. Jin et al. also found that the potential of carbon steel in concrete decreased with the Cl^- concentration from continuous monitoring by MnO_2 sensor [42]. It can be concluded from the OCP results that oleic acid in concrete can inhibit the corrosion of carbon steel.

3.3. Electrochemical impedance spectroscopy (EIS)

The electrochemical impedance plots of the reinforced concrete samples with and without oleic acid inside immersed in 10 wt.% NaCl solution for 3 months and 1 year are shown in **Fig. 4** and **Fig. 5**, respectively.

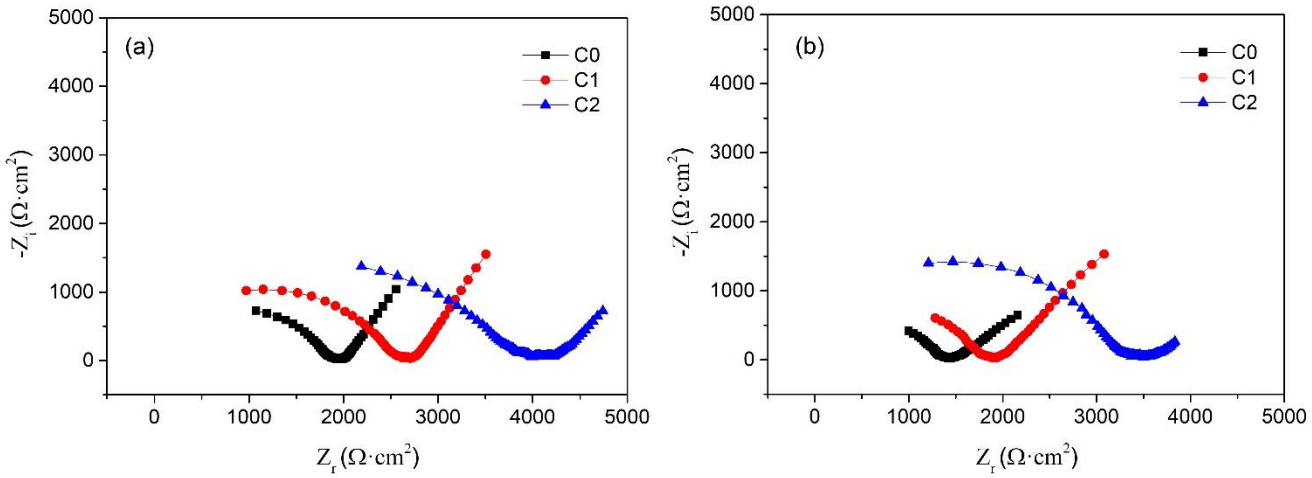

Figure 4. Nyquist plot (a) and Bode plot (b) for the carbon steel electrode in concrete immersed in 10 wt.% NaCl solution for 3 months

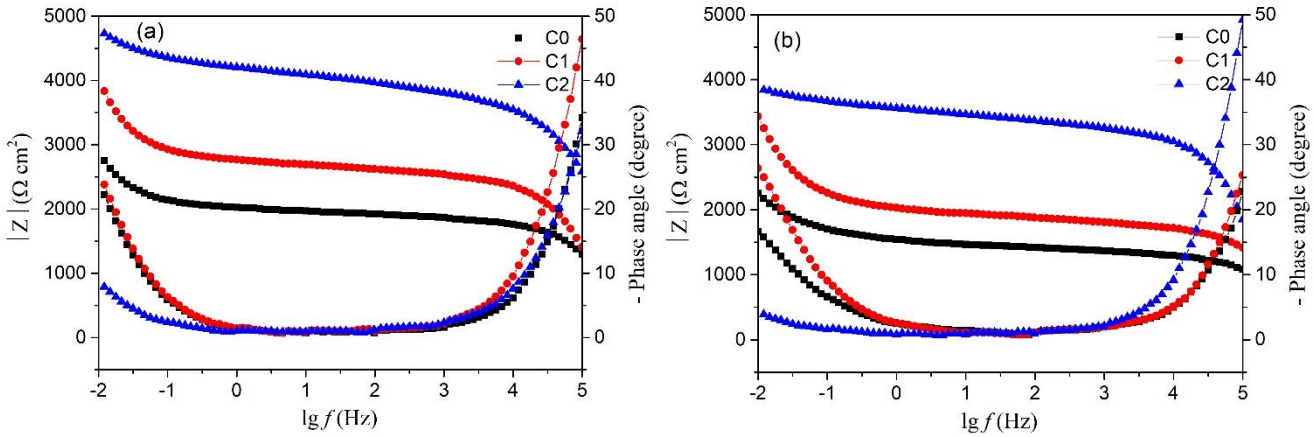

Figure 5. Nyquist plot (a) and Bode plot (b) for the carbon steel electrode in concrete immersed in 10 wt.% NaCl solution for 1 year

The two Nyquist plots show that the position and shape of the circular arc change with the content

of oleic acid in the concrete, indicating that the corrosion resistance of the carbon steel in the concrete with oleic acid increases [43]. The two Bode plots reveal that the impedance modulus and phase angle of the carbon steel corrosion system increase as the oleic acid content increases. It can also be seen in both figures that the corrosion residence of the carbon steel in the concrete decreases as the immersion time increases.

The equivalent circuit model used to analyse the changes in the Nyquist and Bode plots of the corrosion system in detail is shown in **Fig. 6** [44, 45]. The *R*c and *R*ct variables in the model represent the resistance of the concrete cover and the charge transfer during corrosion, respectively. And *C*dl represents the capacitance of the double layer on the surface of the carbon steel.

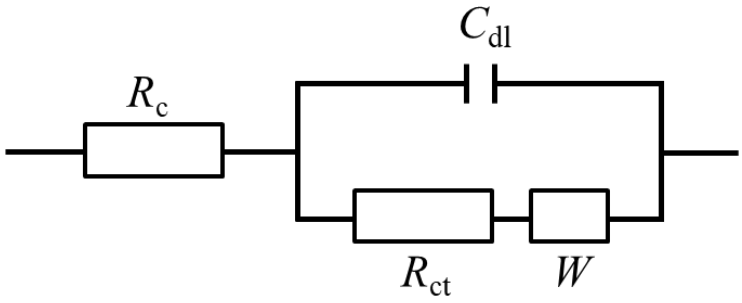

Figure 6. Equivalent circuit model used to fit EIS experiment data

The electrochemical corrosion of metals has different responses to applied electrical signals with different frequencies. Thus, the characteristics of the reactions can be discriminated according to the response of the respective reaction. The high-frequency region of the Nyquist plot of the corrosion system reflects the characteristics of the interface between the concrete and carbon steel, while the low-frequency section indicates the corrosion behaviour of the carbon steel. The fitted *R*c values were 546, 649 and 1454 $\Omega \cdot cm^2$ for the C0, C1 and C2 samples immersed in 10 wt.% NaCl solution for 3 months, respectively. The *R*ct values were 698, 1061 and 2870 $\Omega \cdot cm^2$ for the C0, C1 and C2 samples, respectively, which were immersed in 10 wt.% NaCl solution for 1 year. It can be found that the resistance of the concrete cover and the charge transfer both increase after the addition of oleic acid into the concrete. It is known that the resistance of the concrete cover is related to the electrolyte concentration of the concrete pore solution, the porosity of the concrete and the size and connectivity of the pores [46, 47]. After long-term immersion in the corrosion solution, the electrical resistance of the concrete cover mainly depends on the ion concentration of the internal pore solution [42]. This result indicates that the electrolyte concentration of the concrete pore solution decreases after the addition of oleic acid into the concrete. In other words, the penetration rate of Na^+ and Cl^- from the immersion solution into the concrete is slower. Due to the decrease in Cl^- concentration in the concrete pore solution after the addition of oleic acid into the concrete, the Cl^- concentration on the carbon steel surface must be lower than that of the contrast sample. According to the reported effect of Cl^- concentration on the corrosion behaviour of carbon steel, the corrosion resistance increases and the corrosion current of carbon steel decreases [48].The increased resistance of the charge transfer also revealed that the

corrosion of the carbon steel was inhibited.

3.4. Polarization measurements

The obtained polarization curves of the carbon steel electrode in concrete immersed in 10 wt.% NaCl solution are shown in **Fig. 7**. It can be observed that the changes in the anodic and cathodic polarization plot shapes are indistinct, indicating that the mechanism of the corrosion of carbon steel remains unchanged [49]. In addition, the location of the polarization curves moved toward the current reduction and potential increase direction when more oleic acid was incorporated into the concrete. It can be concluded that the dissolution of the carbon steel in the anode was inhibited and the corrosion rate was reduced significantly [50]. In addition, the inhibition of corrosion of the carbon steel by the oleic acid is related to its content in the concrete.

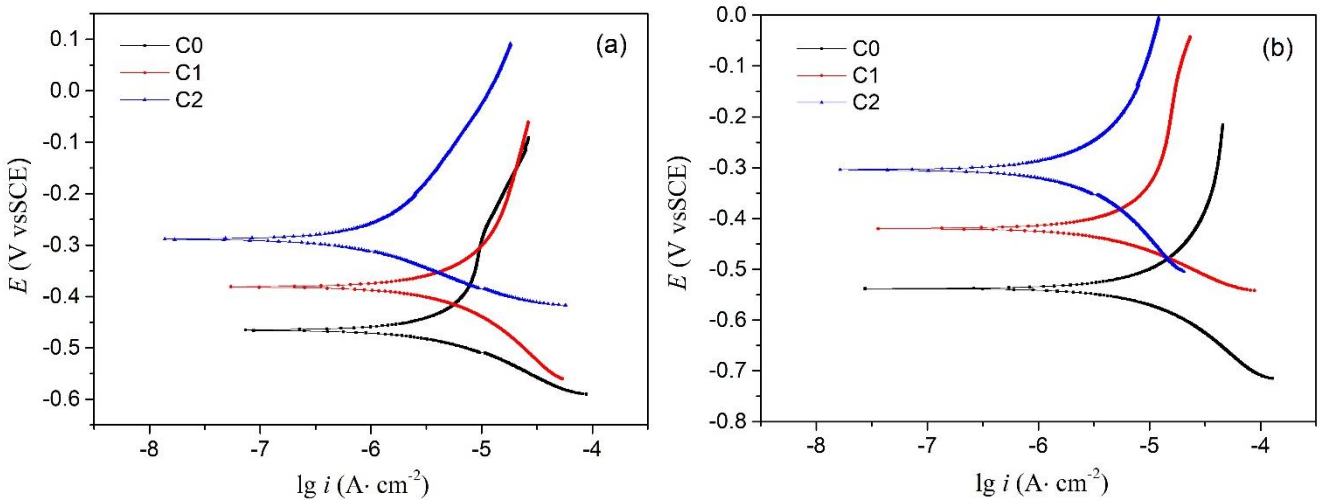

Figure 7. Polarization curves of the carbon steel electrode in concrete immersed in 10 wt.% NaCl solution for 3 months(a) and 1 year(b)

Table 4. Polarization parameters for the carbon steel electrode in concrete immersed in 10 wt.% NaCl solution for 3 months and 1 year

Series	Time	E_{corr} (mV)	β_a (mV dec^{-1})	β_c (mV dec^{-1})	i_{corr} (μA cm^{-2})
C0	3m	-479	854	215	6.08
	1y	-545	350	295	11.30
C1	3m	-357	318	248	2.97
	1y	-436	433	237	5.85
C2	3m	-323	253	217	1.30
	1y	-300	269	221	2.47

To analyse the obtained polarization curves of the carbon steel electrode in concrete in detail, the curves were partly linearly fitted, and the fitted electrochemical parameters, including the corrosion potential (E_{corr}), corrosion current density (i_{corr}), anodic Tafel slope (β_a) and cathodic Tafel slope (β_c), are shown in Table 4. The table shows that i_{corr} decreased with increasing oleic acid content in the concrete, and E_{corr} increased with increasing oleic acid content over the same immersion time. For the same carbon steel electrode in concrete sample, the parameter i_{corr} increased with the immersion time. It can be concluded that the oleic acid in the concrete can effectively decrease the electrolyte concentration of the concrete pore solution. In other words, the penetration rate of the corrosive medium from the immersion solution into the concrete was slower when oleic acid was present [42]. The corrosion trend of the carbon steel increased with the immersion time, which is in agreement with the results from the OCP and EIS tests.

3.5. Cement hydration analysis

To analyse the corrosion inhibition mechanism of oleic acid for carbon steel in concrete, XRD was carried out on pure cement paste and cement paste with added oleic acid. The obtained results are shown in **Fig. 8**. The characteristic peak of the $Ca(OH)_2$ crystal near 18.2° changes with the appearance of oleic acid according to previous study of cement hydration [51]. The peak of the $Ca(OH)_2$ crystal of the pure cement paste sample is sharp, while the peak of the $Ca(OH)_2$ crystal of the cement paste with the oleic acid is shorter and wider at the same diffraction angle position; this difference can be seen clearly in the partial XRD diagram (Fig. 8(b)). The half-peak widths of the $Ca(OH)_2$ crystal peaks of the cement paste samples can be directly calculated by Jade software, and the values are 0.131° and 0.181°. In addition, the crystallinity of the $Ca(OH)_2$ can be estimated by the characteristic peak strength. The results show that the content of the $Ca(OH)_2$ in the cement paste with oleic acid inside is lower than that in the pure cement paste. This result indicates that oleic acid can react with the cement hydration product [40]. In the contact angle test, the contact angle of the hardened cement paste (P0 and P1) increased from 43° to 72°, indicating that some new products with lower surface tension appeared. In addition, the concrete pore structure results indicated that some new products modified the pores, as shown in Table 5. The total porosity and porosity at 500–1600 μm decreased with the amount of oleic acid, indicating that some new products appeared and blocked the concrete pores during the hydration of cement. Similarly, Yang found that thining the pore structure of concrete can decrease the chloride ion migration rate [52].

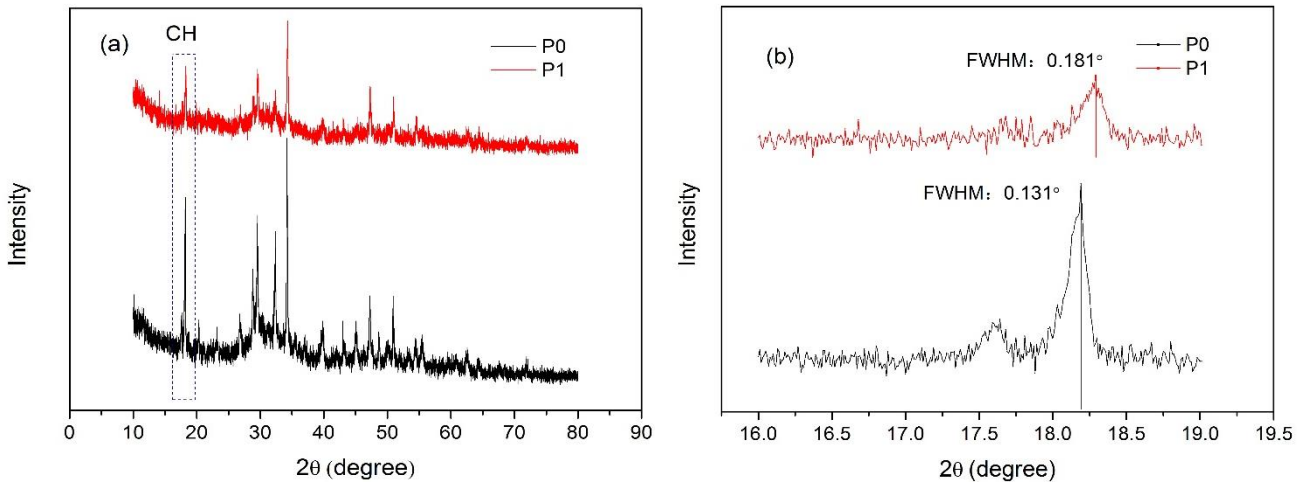

Figure 8. XRD results of the cement paste specimens without and with the oleic acid

Table 5. Porosity and pore-size distribution of concrete

Series	Total porosity/%	Porosity in pore size range/%					
		10-100 *um*	100-200 *um*	200-500 *um*	500-800 *um*	800-1200 *um*	1200-1600 *um*
C0	3.67	0.15	0.42	0.76	0.84	0.81	0.69
C1	2.86	0.25	0.69	0.75	0.53	0.44	0.20
C2	1.87	0.22	0.47	0.52	0.31	0.21	0.14

4. CONCLUSIONS

In this work, the effect of oleic acid on the corrosion resistance of carbon steel in concrete structures was studied systematically. The rapid chloride penetrability test of the concrete samples gave macroscopic and accurate results regarding the inhibition effect of oleic acid on chloride penetration. Electrochemical experiments, including open circuit potential, electrochemical impedance spectroscopy and polarization curves of the corrosion system, were measured to evaluate the inhibition performance of oleic acid on the corrosion of carbon steel. XRD analysis of the cement hydration products was used to study the inhibition mechanism of oleic acid. From the received results, the following conclusions can be drawn:

1. Oleic acid exhibited an excellent inhibitory effect on the penetration of chlorides from the corrosion solution into the concrete. It can effectively increase the resistance of the concrete when the concrete structures are immersed in the corrosion solution.

2. Oleic acid inhibits the corrosion of carbon steel in concrete structures mainly by increasing the corrosion potential, polarization resistance of carbon steel and resistance of the charge transfer process of the corrosion system.

3. The product of the reaction of oleic acid and calcium hydroxide expresses lower surface

tension and blocks the concrete pores. Thus, the penetration of water and chlorides from the outside environment into the concrete can be decreased.

4. Oleic acid performed well in inhibiting the corrosion of the reinforced concrete in the simulated chloride environment. It can potentially be used as an effective inhibitor in reinforced concrete structures that suffer from chloride corrosion.

ACKNOWLEDGEMENTS
Thanks for the financial support provided by Science Foundation of Nanjing Institute of Technology (NO.YKJ201929), the Natural Science Foundation of the Jiangsu Higher Education Institutions of China (NO.20KJB560005) and National Science Foundation of China (NO. 51808369 and 52078247).

References

1. V. Afroughsabet, L. Biolzi and T. Ozbakkaloglu, *J. Mater. Sci.,* 51 (2016) 6517.
2. S. Teng, V. Afroughsabet and C.P. Ostertag, *Constr. Build. Mater.,* 182 (2018) 504.
3. A. Siddika, Md.A.Al Mamun, R. Alyousef and Y.H. Mugahed Amran, *J. Build. Eng.,* 25 (2019) 100798.
4. C. Peng, Q. Wu, J. Shen, R. Mo and J. Xu, *J. Build. Eng.,* 41 (2021) 1.2767.
5. D.Z. Tang, Y. X. Du, M. X. Lu, Z. T. Jiang, L. Dong and J. J. Wang, *Mater. Corros.,* 66 (2015) 278.
6. M. A. Amin, S. S. A. El-Rehim, E.E.F. El-Sherbini and R. S. Bayoumi, *Electrochim. Acta,* 52 (2008) 3588.
7. A.Y. El-Etre, *J. Colloid Inter. Sci.,* 314 (2007) 578.
8. F.B. Ma, W.H. Li, H.W. Tian and B.R. Hou, *Int. J. Electrochem. Sci.,* 10 (2015) 5862.
9. Z.H. Dong, W. Shi and X.P. Guo, *Corros. Sci.,* 53 (2011) 1322.
10. Z.B. Hammouti, H. Zarrok and M. Bouachrine, *Int. J. Electrochem. Sci.,* 7 (2012) 89.
11. Y. Yan, H. Deng, W. Xiao, T. Ou, X. Cao, *Int. J. Electrochem. Sci.,* 15 (2020) 1713.
12. A. Zarrouk, B. Hammouti, R. Touzani, S.S. Al-Deyab, M. Zertoubi, A. Dafali and S. Elkadiri, *Int. J. Electrochem. Sci.,* 6 (2011) 4939.
13. Z. Yang, H. Fischer, J. Cerezo, J.M.C. Mol and R. Polder, *Mater. Corros.,* 67 (2016) 721.
14. R. Ramanauskas, O. Girčienė, L. Gudavičiūtė and A. Selskis, *Appl. Surf. Sci.,* 327 (2015) 131.
15. C. Fang, K. Lundgren, L. Chen and C. Zhu, *Cem. Concr. Res.,* 34 (2004) 2159.
16. T. Vidal, A. Castel and R. François, *Cem. Concr. Res.,* 34 (2004) 165.
17. S. Yoon, K.Wang, W. William and S. Surendra, *ACI Struct. J.,* 97 (2000) 637.
18. A. K. Azad, S. Ahmad and S. A. Azher, *ACI Struct. J.,* 104 (2007) 40.
19. C. Q. Li, R. E. Melchers and J. J. Zheng, *ACI Mater. J.,* 103 (2006) 479.
20. Y. Xi and Z. P. Bažant, *J. Mater. Civ. Eng.,* 11 (1999) 58.
21. F.Z. Zhu, Z.M. Ma, M.M. Zhang, *Adv. Civ. Eng.,* (2020) 1468717.
22. D.Z. Tang, Y. X. Du, M. X. Lu, Z. T. Jiang, L. Dong and J. J. Wang, *Mater. Corros.,* 66 (2015) 278.
23. M. Valcuende, R. Calabuig, A. Martinez-Ibernon, J. Soto, *Materials,* 13 (2020) 5135.
24. H.L. Wang, J.G. Dai, X.Y. Sun and X.L. Zhang, *Constr. Build. Mater.,* 107 (2016) 216.
25. E. Badogiannis, E. Aggeli, V.G. Papadakis and S. Tsivilis, *Cem. Concr. Res.,* 63 (2015) 1.
26. K. Takewaka and S. Mastumoto, *ACI Special Publication,* 109 (1988) 381.
27. C.S. Poon, S.C. Kou and L. Lam, *Constr. Build. Mater.,* 20 (2006) 858.
28. H.W. Song and S.J. Kwon, *Cem. Concr. Res.,* 37 (2007) 909.
29. H.W. Song and S.J. Kwon, *Cem. Concr. Res.,* 39 (2009) 814.
30. S. Lu, E.N. Landis and D.T. Keane, *Mater. Struct.,* 39 (2006) 611.
31. M. Zhang and H. Li, *Constr. Build. Mater.,* 25 (2012) 608.

32. K. Hong and R.D. Hooton, *Cem. Concr. Res.,* 29 (1999) 1379.
33. M.M. Al-Zahrani, S.U. Al-Dulaijan, M. Ibrahim, H. Saricimen and F.M. Sharif, *Cem. Con. Com.,* 24 (2002) 127.
34. A.M.G. Seneviratne, G. Sergi and C.L. Page, *Constr. Build. Mater.,* 14 (2000) 55.
35. H.Y. Moon, D.G. Shin and D.S. Choi, *Constr. Build. Mater.,* 21 (2007) 362.
36. R.N. Swamy and S.T anikawa, *Mater. Struct.,* 26 (1993) 465.
37. R.N. Swamy, A.K. Suryavanshi, and S. Tanikawa, *ACI Mater. J.*, 95 (1998) 101.
38. A.T. Albayrak, M. Yasar, M. A. Gurkaynak and I. Gurgey, *Cem. Concr. Res.,* 35 (2005) 400.
39. S.V. Nanukuttan, L. Basheer, W.J. McCarter, D.J. Robinson, and P.A. Muhammed Basheer, *ACI Mater. J.*, 105(2008) 81.
40. W. J. McCarter, B.T. Linfoot, T.M. Chrisp and G. Starrs, *Mag. Concrete Res.,* 60 (2008) 261.
41. M.J. Al-Kheetan, M.M. Rahman and D.A. Chamberlain, *Struct. Concrete,* 19 (2018) 1504.
42. M. Jin, S. Gao, L. Jiang, Y. Jiang, D. Wu, R. Song, Y. Wu and J. He, *Int. J. Electrochem. Sci.,* 13 (2018) 719.
43. F. Ma, Y. Zhang, H. Wang, W. Li and B. Hou, *Int. J. Electrochem. Sci.,* 13 (2018) 235.
44. A. Ali Gűrten, K. Kayakırılmaz and M.Erbil, *Constr. Build. Mater.,* 21 (2007) 669.
45. H. Zheng, W. Li, F. Ma, Q. Kong, *Cem. Concr. Res.,* 55 (2014) 102.
46. R.D. Moser, P.M. Singh, L.F. Kahn and K.E. Kurtis, *Corros. Sci.,* 57 (2012) 241.
47. G. Sahoo and R Balasubramaniam, *Corros. Sci.,* 50 (2008) 131.
48. T. Ji, F. Ma, D. Liu, X. Zhang, X. Zhang and Q. Luo, *Int. J. Electrochem. Sci.,* 13 (2018) 5440.
49. Q. Li, H. Meng, R., X. Gong, B. Long, R. Ni, X. Gong and J. Dai, *Int. J. Electrochem. Sci.,* 15 (2020) 109.
50. H. Yu, X. Shi, W.H. Harrt and B. Lu, *Cem. Concr. Res.,* 40 (2010) 400.
51. K. Meinhard and R. Lackner, *Cem. Concr. Res.,* 38 (2008) 794.
52. C.C. Yang, *Cem. Concr. Res.,* 36 (2006) 1304.